

**Journal of
Biomimetics, Biomaterials
and Biomedical Engineering**

Table of Contents

Preface

Identification of Bone Density Changes Applying Impedance Spectroscopy with a Piezo-Device Coupled to a Human Tooth J. Ortiz-Jimenez, H.A. Tinoco, C.I. Cardona, J.P. Gomez, F.N. Jiménez-Garcia and S. Roldan-Restrepo	1
Green Synthesis of ZnO Nanoparticles Using <i>Caesalpinia sappan</i> Leaf Extracts and its Antibacterial Activity on <i>Ralstonia solanacearum</i> P.J.G. Eugenio, M.M. Sarong, K.S.A.M. Rapanit, J.C.G.S. Galande, J.F. Nilo and J.J. Monserate	11
Nature-Inspired Nanoflower Structures on Titanium Surface via Alkali Treatment for Biomedical Applications J. Vishnu and G. Manivasagam	20
Responsive Calcium (Ca²⁺) Alginate-Chitosan Based Hydrogel: A Promising Biomaterial for Spinal Cord Injury F. A'yunni, P. Widiyanti and D. Hikmawati	29
Characterization of Indonesia Decellularized Liver Cubes Scaffold using Scanning Electron Microscopy A.A.A.A.P. Dewi, R.D. Antarianto and J.A. Pawitan	38
Development of Aldehyde Hyaluronic Acid - N,O-Carboxymethyl Chitosan based Hydrogel for Intraperitoneal Antiadhesion Application P. Widiyanti, Y.C.A. Priskawati, H. Wibowo and J. Ady	47
Tantalum as a Novel Biomaterial for Bone Implant: A Literature Review I. Putrantyo, N. Anilbhai, R. Vanjani and B. De Vega	55
The Identification of HSA-MIR-17-5P Existence in the Exosome of Adipose-Derived Stem Cells and Adipocytes S. Murlistyarini, L.P. Aninda, U.A. Afridafaz, S. Widyarti, A.T. Endharti and T.W. Sardjono	66
Characterization of Scleraxis and SRY-Box 9 from Adipose-Derived Stem Cells Culture Seeded with Enthesis Scaffold in Hypoxic Condition T. Prajasari, C.M. Zaim and H. Suroto	76
Micro-Computed Tomography Analysis on Administration of Mesenchymal Stem Cells - Bovine Teeth Scaffold Composites for Alveolar Bone Tissue Engineering D.S. Sari, F.D.E. Latief, Ferdiansyah, K. Sudiana and F.A. Rantam	86

Micro-Computed Tomography Analysis on Administration of Mesenchymal Stem Cells - Bovine Teeth Scaffold Composites for Alveolar Bone Tissue Engineering

Desi Sandra Sari^{1,a,*}, Fourier Dzar Eljabbar Latief^{2,b}, Ferdiansyah^{3,5,c},
Ketut Sudiana^{4,d} and Fedik Abdul Rantam^{5,6,7,e}

¹Department of Periodontics, Faculty of Dentistry, Universitas Jember, Jember, Indonesia.

²Micro-CT Laboratory, Faculty of Mathematics and Natural Sciences, Institut Teknologi Bandung, Indonesia.

³Department of Orthopaedics & Traumatology, Dr. Soetomo General Hospital, Surabaya, Indonesia.

⁴Department of Anatomical Pathology, Faculty of Medicine, Universitas Airlangga, Surabaya, Indonesia.

⁵Regenerative Medicine & Stem Cell Centre, Universitas Airlangga & Dr. Soetomo General Hospital, Surabaya, Indonesia.

⁶Stem Cells Research and Development Center, Universitas Airlangga, Surabaya, Indonesia.

⁷Department of Virology, Microbiology, and Immunology, Faculty of Veterinary Medicine, Universitas Airlangga, Surabaya, Indonesia

Email: ^adesi_sari.fkg@unej.ac.id, ^bfourier@fi.itb.ac.id, ^cferdyortho@yahoo.com,
^dik.sudiana@yahoo.com, ^efedik-a-r@fkh.unair.ac.id

*Corresponding author: Desi Sandra Sari, Faculty of Dentistry, University of Jember, Jl. Kalimantan 37 Jember, East Java

Keywords: Mesenchymal Stem Cells, Bovine Teeth, Scaffold, Regeneration, Alveolar Bone, Periodontitis, Micro-computed tomography, 3-Dimensional

Abstract. The tissue engineering approach for periodontal tissue regeneration using a combination of stem cells and scaffold has been vastly developed. Mesenchymal Stem Cells (MSCs) seeded with Bovine Teeth Scaffold (BTSc) can repair alveolar bone damage in periodontitis cases. The alveolar bone regeneration process was analyzed by micro-computed tomography (μ -CT) to observe the structure of bone growth and to visualize the scaffold in 3-Dimensional (3D). The purpose of this study is to analyze alveolar bone regeneration by μ -CT following the combination of MSCs and bovine teeth scaffold (MSCs-BTSc) implantation in the Wistar rat periodontitis model. Methods. MSCs were cultured from adipose-derived mesenchymal stem cells of rats. BTSc was taken from bovine teeth and freeze-dried with a particle size of 150-355 μ m. MSCs were seeded on BTSc for 24 hours and transplanted in a rat model of periodontitis. Thirty-five Wistar rats were made as periodontitis models with LPS induction from *P. gingivalis* injected to the buccal section of interproximal gingiva between the first and the second mandibular right-molar teeth for six weeks. There were seven groups (control group, BTSc group on day 7, BTSc group on day 14, BTSc group on day 28, MSCs-BTSc group on day 7, MSCs-BTSc group on day 14, MSCs-BTSc group on day 28). The mandibular alveolar bone was analyzed and visualized in 3D with μ -CT to observe any new bone growth. Statistical Analysis. Group data were subjected to the Kruskal Wallis test followed by the Mann-Whitney ($p < 0.05$). The μ -CT qualitative analysis shows a fibrous structure, which indicates the existence of new bone regeneration. Quantitative analysis of the periodontitis model showed a significant difference between the control model and the model with the alveolar bone resorption ($p < 0.05$). The bone volume and density measurements revealed that the MSCs-BTSc group on day 28 formed new bone compared to other groups ($p < 0.05$). Administration of MSCs-BTSc combination has the potential to form new alveolar bone.

Introduction

In Indonesia, periodontal disease is a dental and oral health problem often experienced by people in all age groups [1, 2]. Periodontal disease is a chronic inflammatory disease that damages the tissues and structures around the teeth, including the gingiva, cementum, periodontal ligaments, and alveolar bone. The alveolar bone supports the tooth socket (alveoli) and assists the movement of teeth while helping distribute occlusal forces and supplies nutrients to the periodontal ligament; if alveolar bone resorption occurs, it will cause tooth decay and tooth loss. A particular way to treat such an issue is by using a tissue engineering approach [3–5].

Tissue engineering involves mesenchymal stem cells, natural and synthetic scaffolds, and growth factors. MSCs are considered suitable candidates for tissue engineering techniques because MSCs can proliferate and differentiate into several organs' cells [6–8]. The MSCs, combined with the scaffold, can induce the desired tissue formation, causing cell growth in the surrounding area. Ideally, the scaffold should be biocompatible, biodegradable, and non-toxic. Scaffold from bovine teeth is the most widely used replacement material for human teeth and is currently researched in dentistry [9–11]. Research from Sari states that the combination of MSCs and BTSc has osteogenic capability and is non-toxic [12].

Currently, micro-CT for tissue engineering evaluation is rapidly evolving, whether *in vitro*, *in vivo*, and *ex vivo* research. Micro-CT alone cannot completely replace conventional approaches, SEM, or histological examination but may offer significant benefits regarding the non-destructive procedures and direct 3D model structural analysis [13–15].

The micro-CT analysis results on the mandible of Wistar rats showed a morphological picture of alveolar bone resorption, in which there was a decrease of the bone margin in an apical direction [16]. This study analyzed alveolar bone regeneration by micro-CT after combining MSCs and bovine teeth scaffold (MSCs-BTSc) *in vivo*.

Materials and Methods

This research has received approval from the Animal Care and Use Committee from the Faculty of Veterinary Medicine, Airlangga University, Number.637-KE.

Scaffold Characterization

The process of making powder is carried out by inserting cow teeth into a bone miller and crushed so that they come out as particles, then filtered according to the desired size. Before storage, the proteins contained in the teeth were frozen (Freeze-dried = lyophilized) in dry condition (sublimation) in the form of particles. Particles were made in the size of 150-355 μm and sterilized in The National Nuclear Energy Agency of Indonesia (BATAN, Jakarta, Indonesia). Scanning Electron Microscopy (SEM) of bovine teeth particle shape was performed with the magnification of 1500 \times (FK UA Electron Microscope Lab). Micro-computed tomography (μ -CT) imaging and analysis were performed on the particle [12, 17].

Cell Culture and Scaffold Seeding

MSCs from the rat's adipose tissue were extracted retroperitoneally. Then cultured MSCs with alpha-modified Minimum-essential Eagle Medium (α MEM) plus 15% Fetal Bovine Serum (FBS), 2 mM L-glutamine and 100 IU/mL penicillin, 100 mg/mL streptomycin, 2.5 $\mu\text{g}/\text{mL}$ fungizone, incubated at 37°C with 5% CO₂ content, and passaged 4-5 times. Bovine teeth scaffolds were immersed in α MEM medium for 24 hours; the medium was removed and replaced with a new medium. After one day, 5 mg of bovine teeth scaffold was put in 96 culture wells and added with a medium suspension containing 2x 10⁶ and incubated for 1 hour at 37°C and 5% CO₂. Samples were fixed with 4% paraformaldehyde phosphate buffer and 2% osmic acid. After dehydration with water-

ethanol and ethanolisoarnyl acetate solution, the sample was dried with a lyophilizer and then observed with an SEM (Mag.5000, 20.000 kV, WD 10.0 mm, University of Airlangga) [12, 18].

Periodontitis Model

Thirty-five mice were modeled for periodontitis by induction of LPS from *P. gingivalis*, which was injected into the buccal section of interproximal gingiva between the first and second mandibular right-molar teeth. Then we gave each experimental animal LPS from *P.gingivalis* with a volume of 10 μ l and a concentration of 0.5 mg/ml. These models were then analyzed by means of μ -CT imaging technique [19, 20].

Transplant MSCs-BTSc on Periodontitis model

The MSCs-BTSc composite was inserted into the periodontal pocket of the mice. There were seven groups of Wistar rats, namely the control group, the periodontitis model group and the 7th day BTSc, the periodontitis model group and the 14th-day BTSc, the periodontitis model group and given the 28th-day BTSc, the periodontitis model group, and given MSCs-BTSc day 7, the periodontitis model group and given MSCs-BTSc on day 14, the periodontitis model group and given MSCs-BTSc on day 28. The experimental animals were sacrificed on the 7th, 14th, and 28th day and analyzed by μ -CT.

Micro-CT (Micro-Computed Tomography) Analysis

The scanning of the samples was performed using a high-resolution μ CT scanner (SkyScan 1173; Bruker-microCT, K ntich, Belgium), which has an X-Ray source energy of 40-130 kV, which is suitable for scanning the scaffold and the teeth samples. The device produces a microstructural 3D image of the samples by means of X-Ray attenuation. While a minimum of 180  scan rotation is required to produce 3D tomography images, SkyScan 1173 employs a minimum rotation of 240  with an adjustable rotation step according to the selected image resolution. The quality of the raw projection images can be selected accordingly with three available options: high-quality mode (5 to 35 μ m spatial resolution), the medium quality mode (10 to 70 μ m spatial resolution), and the standard quality mode (20 to 140 μ m spatial resolution). The three sets of samples were scanned with the parameters in such a way as to produce a decent contrast ratio and low noise of projection images (see Table 1) [16, 21].

A reconstruction by the NRecon v.1.7.3.1 (Bruker-microCT, K ntich, Belgium) software then follows the scanning process to produce a 3D grayscale image. The Feldkamp back-projection algorithm is implemented in the GPU-based kernel reconstruction using GPUReconServer v.1.7.3.1 (Bruker-microCT, K ntich, Belgium), which is preferred due to its capability of using the GPU cores to accelerate the reconstruction process. The NRecon software can also compensate several artifacts such as misalignment, ring artifact, and beam hardening effect to improve the quality of the produced 3D structure of the samples [22, 23].

Post reconstruction, a greyscale 3D image is obtained as a series of trans-axial (*x-y* plane) 2D images where the grayscale level is correlated with the sample's density. Bright areas indicate denser parts of the sample, while darker areas indicate the lower ones. Qualitative analysis can be done by visual inspection using DataViewer, which can visualize the sample in ortho-slice view. DataViewer can also be used to perform sample reorientation to produce aligned 3D images, in addition to color-coding, Volume of Interest (VOI) selection, and image registration in 2D and 3D. A more thorough inspection can be done using 3D visual, which was done using CTVox v.3.3 (Bruker-microCT, K ntich, Belgium). Several 3D manipulations such as 3D rotation, object slicing, cropping, and clipping can be done without altering the original dataset. The contrast and brightness of the 3D visual can also be adjusted to inspect and isolate specific sample compositions of different densities [24, 25].

Table 1. Scanning parameters for the three sets of samples

Parameter	Value		
	Bovine teeth scaffold	Periodontitis model	Transplanted samples
Energy [kV]	40	60	60
Current [μ A]	130	106	106
Exposure time [ms]	500	250	250
Filter type	Al 1.0 mm	Al 1.0 mm	Al 1.0 mm
Rotation step [$^{\circ}$]	0.2	0.2	0.2
Camera binning	1 \times 1	2 \times 2	2 \times 2
Dimension of proj. image	2240 \times 2240	1120 \times 1120	1120 \times 1120
Raw image res. [μ m/pixel]	5.70	19.95	19.95

The Micro-CT imaging technique provides the ability to analyze a sample without physically altering the sample through image processing and analysis. Two necessary image processing needs to be conducted firstly, i.e., defining a Volume of Interest (VOI) for the 3D analysis and the structure segmentation (through thresholding) to differentiate the object of interest and the background (or often referred to as void). Numerous automated (objective, algorithm-based) thresholding methods are available in CTAn (CT Analyser) software v.1.20.8.0+ (Bruker-microCT, K ntich, Belgium). However, due to the complexity of the observed samples, manual threshold selection was used for consistency. Afterward, measurements of several characteristics of the sample can be done by means of image analysis. Table 2 shows the relevant measured morphometric parameters that were calculated in this study using CTAn, i.e., the Object Volume and the Structure Thickness (for particle size analysis). The nomenclature used in this research is based on the American Society for Bone and Mineral Research (ASBMR). Other than these parameters, the periodontitis model's relative density and the transplanted samples were analyzed using the mean Grayscale Index (GS.Idx) inside the defined VOI [15, 26].

Table 2. Some typically calculated morphometric parameters for life-science-related samples

Parameter name, symbol, and unit		Brief description
General Scientific	Bone ASBMR	
Object volume, Obj.V, mm ³	Bone volume, BV, mm ³	The total volume of binarised objects within the VOI, measured based on the marching cubes volume model of the binarised objects within the VOI.
Structure Thickness, St.Th, mm	Trabecular Thickness, Tb.Th, mm	A measurement of the solid structure's thickness based on the maximum sphere from the medial axis.

Statistical Analysis

Data analysis was performed using descriptive statistics. The data were analyzed using the kruskal wallis test and followed by Mann-Whitney ($p < 0,05$).

Result and Discussion

The scanning process produces a series of raw projection images in 16-bit TIFF image format. Subsequently, the raw projection images were then reconstructed to produce 8-bit grayscale BMP images. The 2D, ortho-slice, and 3D images of the bovine teeth scaffold are displayed in Figure 1. Figure 1.a. shows the results from the reconstruction process, visualized by DataViewer v.1.5.6.2. (Bruker-microCT, K ntich, Belgium) as trans-axial, coronal, sagittal, and ortho-slice (Figure 1.b.). The

grayscale level can be visually enhanced by applying a colormap that describes the relative density of the materials composing the sample: greenish areas indicate the denser object, and purple-ish is the opposite. Three-dimensional volume rendering in Figure 1.c. is generated using CTVOx shows a visual of the heterogeneous-shaped particles. Further analysis from the μ -CT image of the bovine teeth scaffold reveals particles' formation (grain-like structure) which is interwoven by a fibrous-like structure. Individual particle analysis of the grain-like structure shows a particle size distribution in the range of 5-360 μm (Figure 1.d.) with a mean particle size of 151 μm .

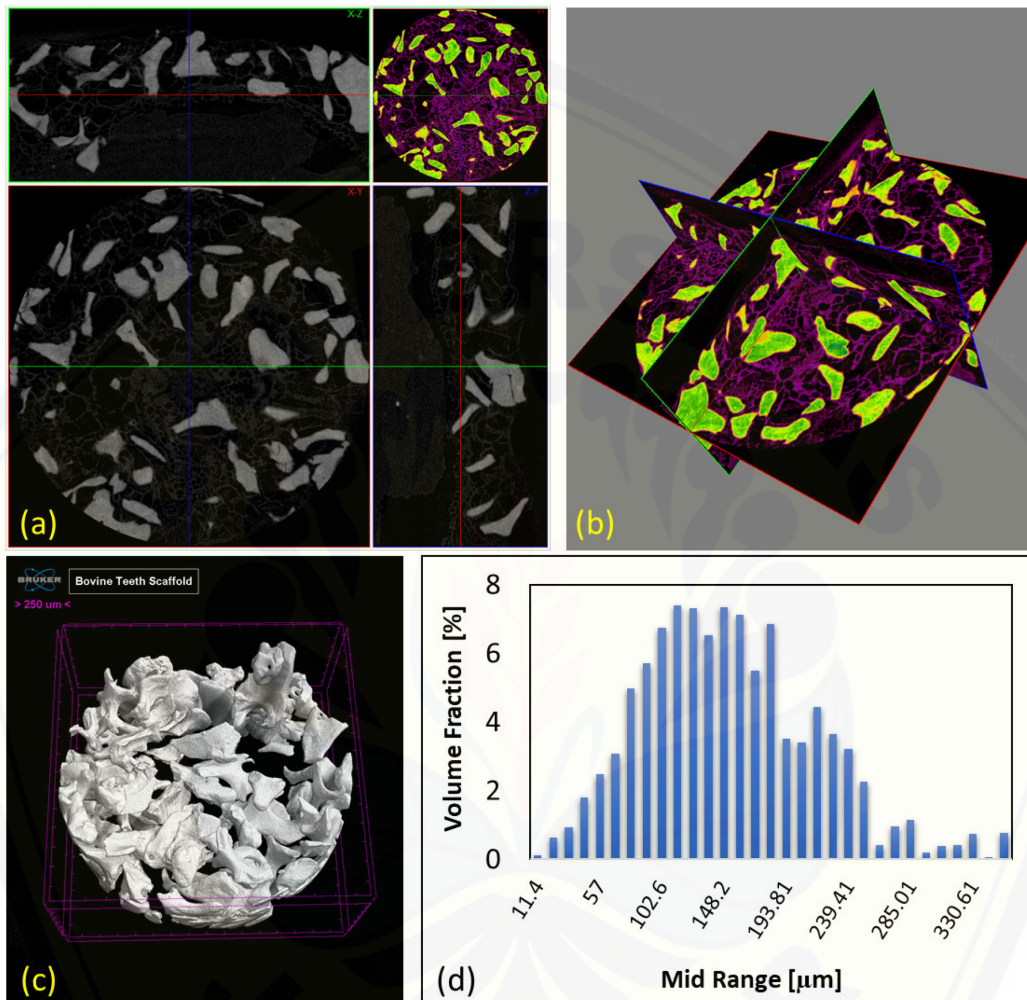


Figure 1. Images of bovine teeth scaffold (a) 2D slices (grayscale and color-enhanced) (b) ortho-slice view (c) 3D view (d) Particle size distribution

The size of the bovine teeth scaffold in this study was 150-355 μm . The MSCs were seeded on scaffolds with pore sizes ranging from 200 - 750 μm . This size is recommended because resorption takes a long time if the particle size is too large, and particles are resorbed before they can serve as a graft material if the size is too small. The particle size of the graft material affects bone formation. However, several animal studies have shown that bovine teeth scaffolds are biocompatible and osteoinductive [27–29]. Previous studies stated that collagen combined with demineralized bone powder with a particle size of 250-500 μm is suitable for osteoblast differentiation environments and has the potential for bone tissue engineering [30].

Ceramic scaffolds with pore sizes of 200 μm and 500 μm have a relatively higher ability of osteogenic differentiation, whereas scaffolds with pores of 380–405 μm have a more increased osteoblast proliferation, while those in the range of 186–200 μm are more suitable for fibroblast proliferation [13, 15].

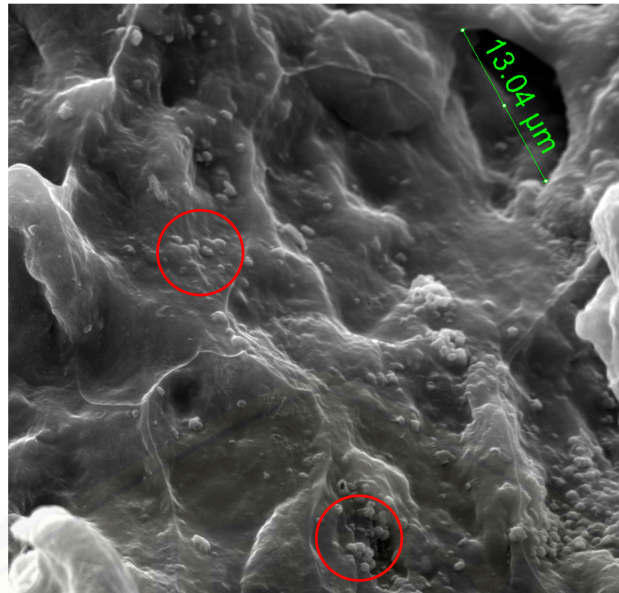


Figure 2. The result of MSCs seeding into the bovine teeth scaffold for 24 hours, marked with a red circle (Mag.5000×)

SEM results showed that the number of cells attached to the bovine teeth' scaffold surface increased after 24 hours of seeding compared to 1 hour and 12 hours (unpublished data). Cell proliferation results indicate that the bovine teeth scaffold is suitable for the cell environment and supports cell growth and cell proliferation, and differentiation [18, 31]. Yamanaka et al. (2015) research results that MSCs were fed into HAP / PLGA blocks for 12 hours, and high seeding efficiency results (up to 90%) could be achieved for a short time of 12 hours [32]. SEM analysis shows that a formation has appeared on the surface of the bovine teeth scaffold with a diameter of 4,864 μm, which indicates exposed dentinal tubules, thus providing a channel for releasing proteins, growth factors, and cell adhesions [33].

This study used Wistar rats made a periodontitis model by induction of LPS *P.gingivalis* 3 times a week for six weeks. μ-CT was utilized for this in-vivo evaluation of alveolar bone resorption. The μ-CT analysis revealed the mean alveolar damage induced by LPS of *P.gingivalis*. The result of *P.gingivalis* LPS induction showed alveolar bone resorption up to 1/3 apical (Fig 3) [34].

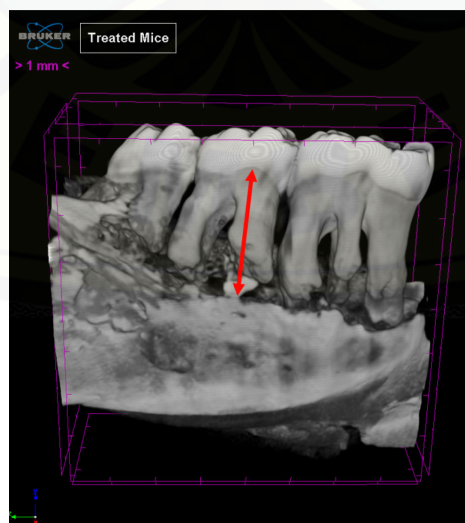


Figure 3. μ-CT imaging in the treated mice (the arrow indicates the cemento-enamel junction (CEJ) and alveolar bone crest (ABC))

On the 7th, 14th and the 28th days, each specimen from the BTSc and the MSCs-BTSc composite were scanned using the μ -CT to analyze new tissue formation. A VOI was selected over the area, which shows new tissue formation, indicated by a distinctive structure, i.e., porous and fibrous-like. The new tissue structure has a particular density compared to the surrounding structure, which was indicated by a distinctive color range when visualized in CTAn. Figure 4 shows the 3D visuals of the samples where the red structures are the newly formed tissues. The further calculation of the structural quantities (the volume and bone density) is shown in Table 1. Bone density is expressed in the Grayscale Index (GS.Idx), representing relative density. GS.Idx has a value range of 0-255, where 0 represents the lowest density (air), and 255 represents the highest density (equivalent to compact bone) [35, 36].

Table 3. Bone volume and density measurement result in each transplant treatment

No	Sample	Volume [Mm ³]	Bone Density
1	BTSc transplant, day 7	not observed	
2	MSCs-BTSc composite transplant, day 7	not observed	
3	BTSc transplant, day 14	0.476	130.563
4	MSCs-BTSc composite transplant, day 14	0.604	133.723
5	BTSc transplant, day 28	1.945	142.378
6	MSCs-BTSc composite transplant, day -28	1.969*	144.158**

From Table 3, it can be observed that the alveolar bone volume was more significant in the MSCs-BTSc composite group than the control group, the treatment group, and the BTSc group alone. Bone density was also denser in the treated group with MSCs-BTSc composite than the other groups. MSCs have begun to differentiate towards osteogenic on the first day, then on the 7th and 11th day, Alkaline phosphatase activity increases five times in bone formation in vivo [37]. Administration of BTSc on day 28 showed an effect on alveolar bone regeneration. The results of the μ -CT analysis showed that there was new bone growth on the 28th day after administering MSCs-BTSc.

Giving bovine teeth scaffold in vivo can improve osteoconduction and osteoinduction functions facilitating endogenous osteoprogenitor cells to migrate, proliferate, adhesion, differentiate and regenerate new bone [38]. Research with μ -CT analysis also showed that at eight weeks, there was a new bone formation by administering tooth grafts on the iliac bone [39].

Previous studies demonstrated the combination of Periodontal Ligament Stem Cells (PDLSCs) from mice with Platelet-Rich Fibrin (PRF) transplanted into alveolar bone defects of the buccal section of mandibular first molars of rats using burs. After the 12th and 24th days after the transplant, the μ -CT examination showed a new periodontal ligament formation. There were new cementum and alveolar bone on the 24th day compared to control and treatment using PRF alone [40]. A study by Akita et al., 2016 showed the μ -CT examination on the formation of new hard tissue in alveolar bone defects in mice after being transplanted with composite Adipose-Derived Mesenchymal Stem Cells (ADMSCs) and scaffold Poly d, L-lactic-co-Glycolic Acid (PLGA) at week 14 [41].

Interestingly, cortical bone tissue was formed in the outer layer after 28 days in the combined Dedifferentiation Fat cells (DFAT cells) and PLGA scaffold groups. The formation of new hard tissue from the mesial to the distal cortical bone in the DFAT/PLGA group happened after the 35th day. There was a translucent image between tooth roots and new hard tissue in all groups on the 35th day [41].

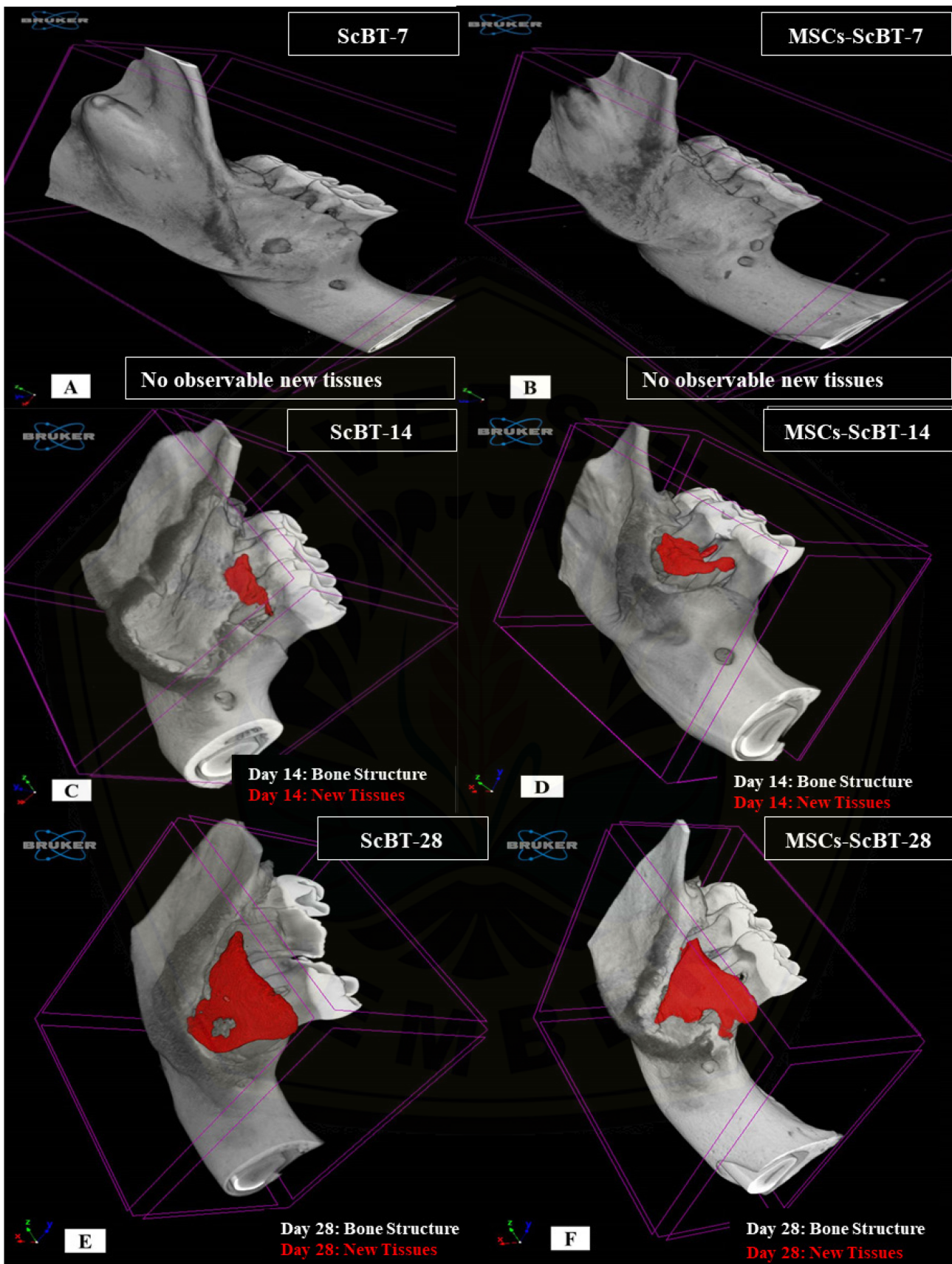


Figure 4. Micro-CT 3D visualizations of alveolar bone defect (A) Transplantation of BTSc day 7, (B) Transplantation of MSCs-BTSc day 7, (C) Transplantation of BTSc day 14, (D) Transplantation of MSCs-BTSc of day 14, (E) Transplantation of BTSc day 28, (F) Transplantation of MSCs-BTSc day 28

Conclusion

MSCs-BTSc composite with BTSc particle size of 150-355 μm has the potential to aid the growth of woven bone and the regeneration of alveolar bone on the 28th day in the periodontitis modeled rat.

Acknowledgment

The author would like to thank The Central Laboratory of Mathematics and Natural Sciences, State University of Malang for providing the SEM.

Conflict of Interest

The authors declare no conflict of interest in the conduct of this study.

References

- [1] Tonetti MS, Jepsen S, Jin L, et al. Impact of the global burden of periodontal diseases on health, nutrition, and wellbeing of mankind: A call for global action. *J Clin Periodontol* (2017) 44: 456–462.
- [2] Shewale AH, Gattani DR, Bhatia N, et al. Prevalence of periodontal disease in the general population of India-A systematic review. *J Clin Diagnostic Res* (2016) 10: ZE04–ZE09.
- [3] Graves DT, Li J, Cochran DL. Inflammation and uncoupling as mechanisms of periodontal bone loss. *Crit Rev Oral Biol Med* (2011) 90: 143–153.
- [4] Intini G, Katsuragi Y, Kirkwood KL, et al. Alveolar bone loss: mechanisms, potential therapeutic targets, and interventions. *Adv Dent Res* (2014) 26: 38–46.
- [5] Chahboun H, Arnau MM, Herrera D, et al. Bacterial profile of aggressive periodontitis in Morocco: a cross-sectional study. *BMC Oral Health* (2015) 15: 25.
- [6] Sun H, Yang HL. Calcium phosphate scaffolds combined with bone morphogenetic proteins or mesenchymal stem cells in bone tissue engineering. *Chin Med J (Engl)* (2015) 128: 1121–1127.
- [7] Abdel Meguid E, Ke Y, Ji J, et al. Stem cells applications in bone and tooth repair and regeneration: New insights, tools, and hopes. *J Cell Physiol* (2018) 233: 1825–1835.
- [8] Requicha JF, Viegas CA, Muñoz F, et al. A Tissue Engineering Approach for Periodontal Regeneration Based on a Biodegradable Double-Layer Scaffold and Adipose-Derived Stem Cells. *Tissue Eng Part A* (2014) 20: 2483–2492.
- [9] Teruel; Dios J De, Alcolea A, Hernandez A, et al. Comparison of chemical composition of enamel and dentine in human, bovine, porcine and ovine teeth. *Arch Oral Biol* (2015) 60: 768–775.
- [10] Abou Neel EA, Chrzanowski W, Salih VM, et al. Tissue engineering in dentistry. *J Dent* (2014) 42: 915–928.
- [11] Yassen GH, Platt JA, Hara AT. Bovine teeth as substitute for human teeth in dental research: a review of literature. *J Oral Sci* (2011) 53: 273–282.
- [12] Sari DS, Setiawatie EM, Mahyudin F, et al. Cytotoxicity test and characteristics of demineralized dentin matrix scaffolds in adipose-derived mesenchymal stem cells of rats. *Dent J* (2018) 194: 194–199.
- [13] Bartoš M, Suchý T, Tonar Z, et al. Micro-CT in tissue engineering scaffolds designed for bone regeneration: Principles and application. *Ceram - Silikaty* (2018) 62: 194–199.
- [14] Bishop ES, Mostafa S, Pakvasa M, et al. 3-D bioprinting technologies in tissue engineering and regenerative medicine: Current and future trends. *Genes Dis* (2017) 4: 185–195.

- [15] Cengiz IF, Oliveira JM, Reis RL. Micro-CT - A digital 3D microstructural voyage into scaffolds: A systematic review of the reported methods and results. *Biomater Res* (2018) 22: 1–11.
- [16] Latief, D E, Sari DS, Fitri L. Applications of Micro-CT scanning in medicine and dentistry : Microstructural analyses of a Wistar Rat mandible and a urinary tract stone Applications of Micro-CT scanning in medicine and dentistry : Microstructural analyses of a Wistar Rat mandible and a. *J Phys Conf Ser* (2017) 884: 0–11.
- [17] Um I-W, Kim Y-K, Mitsugi M. Demineralized dentin matrix scaffolds for alveolar bone engineering. *J Indian Prosthodont Soc* (2017) 17: 120–127.
- [18] Sari DS, Maduratna E, Ferdiansyah, et al. Osteogenic Differentiation and Biocompatibility of Bovine Teeth Scaffold with Rat Adipose-derived Mesenchymal Stem Cells. *Eur J Dent* (2019) 13: 206–212.
- [19] Xing H, Taguchi Y, Komasa S, et al. Effect of *Porphyromonas gingivalis* Lipopolysaccharide on Bone Marrow Mesenchymal Stem Cell Osteogenesis on a Titanium Nanosurface. *J Periodontol* (2015) 86: 448–455.
- [20] Struillou X, Boutigny H, Soueidan A, et al. Experimental animal models in periodontology: a review. *Open Dent J* (2010) 4: 37–47.
- [21] Tayman MA, Kamburoğlu K, Küçük Ö, et al. Comparison of linear and volumetric measurements obtained from periodontal defects by using cone beam-CT and micro-CT: an in vitro study. *Clin Oral Investig* (2019) 23: 2235–2244.
- [22] Radetic T. Fundamentals of scanning electron microscopy and energy dispersive X-ray analysis in SEM and TEM. *NFMC Spring School on Electron Microscopy* (2011):1-52
- [23] Furfaro F, Ang ESM, Lareu RR, et al. A histological and micro-CT investigation in to the effect of NGF and EGF on the periodontal, alveolar bone, root and pulpal healing of replanted molars in a rat model - a pilot study. *Prog Orthod* (2014) 15: 1–12.
- [24] Park HJ, Min KD, Lee MC, et al. Fabrication of 3D porous SF/ β -TCP hybrid scaffolds for bone tissue reconstruction. *J Biomed Mater Res - Part A* (2016) 104: 1779–1787.
- [25] Park JY, Chung JH, Lee JS, et al. Comparisons of the diagnostic accuracies of optical coherence tomography, micro-computed tomography, and histology in periodontal disease: An ex vivo study. *J Periodontal Implant Sci* (2017) 47: 30–40.
- [26] Boerckel JD, Mason DE, McDermott AM, et al. Microcomputed tomography: Approaches and applications in bioengineering. *Stem Cell Res Ther* (2014) 5: 1–12.
- [27] Michel J, Penna M, Kochen J, et al. Recent Advances in Hydroxyapatite Scaffolds Containing Mesenchymal Stem Cells. *Stem Cells Int* (2015) 2015: 1–13.
- [28] Kim Y, Lee J, Um I, et al. Tooth-derived bone graft material. *J Korean Assoc Oral Maxillofac Surg* (2013) 39: 103–111.
- [29] Koga T, Minamizato T, Kawai Y, et al. Bone Regeneration Using Dentin Matrix Depends on the Degree of Demineralization and Particle Size. *PLOS one* (2016) 1–12.
- [30] Thitiset T, Damrongsakkul S, Bunaprasert T, et al. Development of Collagen/Demineralized Bone Powder Scaffolds and Periosteum-Derived Cells for Bone Tissue Engineering Application. *Int J Mol Sci* (2013) 14: 2056–2071.
- [31] Supronowicz P, Gill E, Trujillo A, et al. Human Adipose-Derived Side Population Stem Cells Cultured on Demineralized Bone Matrix for Bone Tissue Engineering. *Tissue Eng Part A* (2011) 17: 789–798.

- [32] Yamanaka K, Yamamoto K, Sakai Y, et al. seeding of mesenchymal stem cells into inner part of interconnected porous biodegradable scaffold by a new method with a filter paper. *Dent Mater J* (2015) 34: 78–85.
- [33] Oliveira GS De, Miziara MN, Silva ER, et al. Enhanced bone formation during healing process of tooth sockets filled with demineralized human dentine matrix. *Aust Dent J* (2013) 58: 326–332.
- [34] Wahyukundari MA, Sari DS, Pujiastuti P, et al. Virulence Comparison Between *Aggregatibacter Actinomycetemcomitans* and *Porphyromonas Gingivalis*: Micro-Computed Tomography (μ -CT) and Inflammatory Cytokines Analysis. *11th International Dentistry Scientific Meeting* (2017): 312-321
- [35] Wu S, Wang J, Zou L, et al. A three-dimensional hydroxyapatite/polyacrylonitrile composite scaffold designed for bone tissue engineering. *RSC Adv* (2018) 8: 1730–1736.
- [36] Turnbull G, Clarke J, Picard F, et al. 3D bioactive composite scaffolds for bone tissue engineering. *Bioactive Materials* (2018) 3: 278–314.
- [37] Prins HJ, Braat AK, Gawlitta D, et al. In vitro induction of alkaline phosphatase levels predicts in vivo bone forming capacity of human bone marrow stromal cells. *Stem Cell Res* (2014) 12: 428–440.
- [38] Tollemar V, Collier ZJ, Mohammed MK, et al. Stem cells, growth factors and scaffolds in craniofacial regenerative medicine. *Genes Dis* (2015) xx: 1–16.
- [39] Nampo T, Watahiki J, Enomoto A, et al. A New Method for Alveolar Bone Repair. *J Periodontol* (2010) 81: 1264–1272.
- [40] Duan X, Lin Z, Lin X, et al. Study of platelet-rich fibrin combined with rat periodontal ligament stem cells in periodontal tissue regeneration. *J Cell Mol Med* (2018) 22: 1047–1055.
- [41] Akita D, Kano K, Saito-Tamura Y, et al. Use of rat mature adipocyte-derived dedifferentiated fat cells as a cell source for periodontal tissue regeneration. *Front Physiol* (2016) 7: 1–12.